ACS Sustainable Chemistry & Engineering

Research Article

pubs.acs.org/journal/ascecg

Biobased Poly(lactide)/ethylene-*co*-vinyl Acetate Thermoplastic Vulcanizates: Morphology Evolution, Superior Properties, and Partial Degradability

Piming Ma,*[,†] Pengwu Xu,[†] Yinghao Zhai,[‡] Weifu Dong,[†] Yong Zhang,[‡] and Mingqing Chen*[,†]

[†]The Key Laboratory of Food Colloids and Biotechnology of Ministry of Education, School of Chemical and Material Engineering, Jiangnan University, 1800 Lihu Road, Wuxi 214122, China

[‡]School of Chemistry and Chemical Engineering, Shanghai Jiao Tong University, Shanghai 200240, China

Supporting Information

ABSTRACT: Partially biobased thermoplastic vulcanizates (TPV) with novel morphology, superior properties and partial degradability were prepared by dynamic cross-link of saturated poly(lactide) and ethylene-*co*-vinyl acetate (PLA/EVA) blends using 2,5-dimethyl-2,5-di(*tert*-butylperoxy)hexane (AD) as a free radical initiator. EVA showed higher reactivity with free radicals in comparison with PLA, leading to much higher gel content of the EVA phase ($G_{f\text{-}EVA}$) than that of the PLA phase ($G_{f\text{-}PLA}$). However, the $G_{f\text{-}PLA}$ increased more steeply at AD content larger than 1 wt % where the reaction of EVA approached to a saturation point. The competing reaction changed the viscosity ratio of the two components (η_{PLA}/η_{EVA}) that resulted in a novel morphology evolution of the TPV, i.e., from sea−island-type morphology to phase inversion via a dual-continuous network-like transition and finally cocontinuity again with increasing the AD content. The cross-link and phase inversion considerably enhanced the melt viscosity (η^*), elasticity (G') and the solid-like behavior of the PLA/EVA-based TPV. Meanwhile, superior tensile strength (σ_t = 21 MPa), low tensile set (T_s = 30%), moderate elongation (ε_b = 200%) and suitable stiffness (E' = 350 MPa, 25 °C) were successfully achieved by tailoring the cross-link structure and phase morphology. In addition, the TPV are partially degradable in aqueous alkali. A degradation rate of approximately 5 wt % was achieved within 10 weeks at 25 °C and the degradation mechanism was investigated from both molecular and macroscopic levels. Therefore, this work provides a new type of partially biobased and degradable materials for substitution of traditional TPV.

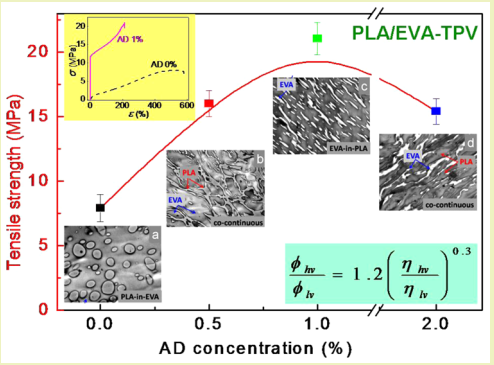

KEYWORDS: *Thermoplastic vulcanizate, Dynamic cross-link, Morphology, Property, Degradation*

INTRODUCTION

Thermoplastic elastomers (TPEs) such as styrene-*b*-butylene-*b*-styrene (SBS) and styrene-*b*-(ethylene-*co*-butylene)-*b*-styrene (SEBS) copolymers possess both rubber-like and thermoplastic behavior.[1,2] A highly engineered class of TPE is the so-called thermoplastic vulcanizates (TPV) that refer to selectively vulcanizing rubber phase upon melt compounding with an immiscible thermoplastic, leading to typical sea−island-type structures where the cross-linked rubber is usually the "island" phase. TPV exhibits advantages in comparison with rubber materials such as reusable after disposal, fast processing and energy saving in the process.[3,4]

The most commercialized TPV so far is the propylene/ethylene-propylene-diene (PP/EPDM) compounds which have been successfully used in the auto industry.[5,6] EPDM is a synthetic rubber with a small fraction of −C═C− bonds that facilitate the selective cross-link of the rubber phase. For this reason, the fabrication of TPV is limited to unsaturated rubbers such as EPDM, natural rubber (NR) and styrene−butadiene rubber (SBR) whereas the plastic matrix is usually chosen from polyolefin.[7−11] On the other hand, traditional TPVs are fully derived from petroleum resources and are nondegradable. This is not preferably designed in terms of sustainability and environmental protection.

Poly(lactide), PLA, is a biobased and biodegradable polymeric material. It is regarded as one of the most promising biopolymers also due to the superior physical-mechanical properties, easy processability and relatively low cost.[12] Thus, PLA is designable for the plastic phase of a new type of TPV. Chen et al.[13] prepared PLA/NR blends via a dynamic cross-link technique. In their study, the NR dosage was below 40 wt % and the cross-linked NR phase owned a continuous network-like dispersion. Liu et al.[14] reported a biobased and supertough TPV consisting of 80 wt % PLA, 20 wt % unsaturated aliphatic polyester elastomer (UPE) and initiator. However, both of the

Received: May 25, 2015
Revised: July 16, 2015
Published: July 22, 2015

DOI: 10.1021/acssuschemeng.5b00462
ACS Sustainable Chem. Eng. 2015, 3, 2211−2219

dynamically cross-linked PLA/NR and PLA/UPE compounds are more like plastics rather than vulcanizates.

On the other hand, ethylene-*co*-vinyl acetate, EVA, is a petroleum-based copolymer that, however, can also be made from renewable resources because both biobased ethylene (e.g., Braskem, Brazil) and biobased vinyl acetate (e.g., Wacker, Germany) are already available on the market. EVA changes from thermoplastic to rubber and then to thermoplastic again with increasing the vinyl acetate (VAc) content from 0 to 100 wt %. Rubber grade EVA (e.g., Levapren EVM) is a saturated copolymer but shows high activity with peroxide.[15] Cassagnau et al.[16] studied the effect of processing conditions on phase inversion of EVA/PP-based TPV via transesterification with tetraethyloxysilane. By the same mechanism, poly(amide)/EVA-based TPV with dispersion of cross-linked EVA phase was prepared and the resulting tensile strength and elongation at break of the poly(amide)/EVA-based TPV were up to 10.6 MPa and 296%, respectively.[17] It is known that properties of TPV are not only influenced by composition and structure but also the compatibility between the components. The compatibility between EVA and PLA can be tuned easily by varying composition of the EVA,[18] thus they might be a good combination for TPV application. Previously, PLA/EVA-based TPV was prepared in our group via a two-step compounding technology in which the initiator (dicumyl peroxide) was premixed with EVA rubber at 90 °C to reduce the reaction possibility of PLA in the subsequent melt compounding at elevated temperatures.[19] Although the two-step compounding could reduce the reaction possibility of PLA to a certain extent it is time and energy consuming in process. Thus, it would be of interest to investigate a more facilitate way to prepare degradable and biobased thermoplastic vulcanizates.

In this work, PLA/EVA-based TPV with novel morphology and superior properties were successfully prepared via an one-step melt compounding in the presence of 2,5-dimethyl-2,5-di(*tert*-butylperoxy)hexane (AD). The prime objective is to provide a deep insight in the competitive reaction between the saturated PLA and EVA phases and the mechanisms of phase inversion. The rheology, (dynamic) mechanical properties and *in vitro* degradation behavior of the TPV are discussed in detail, and the structure−property relationship is investigated.

EXPERIMENTAL SECTION

Materials. Poly(lactide) (PLA, Ingeo 2003D) was purchased from Nature Works LLC, USA, with a melt flow index (MFI) of 3.25 g/10 min (190 °C, 2.16 kg). The content of L-lactide in the PLA is about 96%. Rubber grade EVA (Levapren EVM500) with vinyl acetate (VAc) content of 50 wt % was supplied by Lanxess Chemical Co., Ltd., Qingdao, China. The Mooney Viscosity (100 °C) of the EVA is 27 ± 4 MU. Chloroform and 2,5-dimethyl-2,5-di(*tert*-butylperoxy)hexane (AD, purity of 93%) with a typical half-life time of approximately 6 min at 170 °C were supplied by Heowns Biochem LLC, China. All chemicals were used as received.

Sample Preparation. The PLA and EVA were dried overnight in a vacuum oven at 80 and 40 °C, respectively, before use. They were premixed at 170 °C in a mixer with Roller rotors (RM-200, HABO, China) for 8 min at a rotation speed of 30 rpm to form a homogeneous PLA/EVA compound. Then different amounts of AD (0−3 wt % based on EVA) were fed into the PLA/EVA mixture and kept on rotation at 50 rpm and 170 °C for another 20 min where dynamic cross-link was carried out. The weight ratio of PLA/EVA was fixed at 40/60 (w/w). The samples were finally compression molded into sheets (1 mm in thickness) at 170 °C for 3 min using a compression molding machine for characterizations. All compositions in this work refer to weight ratio.

Characterization. *Cross-Link Structure Analysis.* The cross-link structures of the TPV were studied by swelling equilibrium experiments at 30 °C. Specimens (2 × 1 × 0.5 mm) of each sample were accurately weighted (M_0) and then immersed in chloroform for 72 h to reach a swelling equilibrium. The swollen specimens were taken out, wiped and weighted immediately to an accuracy of 0.1 mg at a given time (M_1). The swollen specimens were then dried in a vacuum oven at 60 °C until the mass change of less than 0.1 mg. The dried residuals, defined as "gel" in this work, were then weighted to an accuracy of 0.1 mg (M_2). The overall gel fraction (G_f) of the TPV was calculated via eq 1, i.e.,

$$G_f = M_2/M_0 \times 100\% \quad (1)$$

Then the gel fraction of the individual PLA phase ($G_{f\text{-PLA}}$) is calculated via eq 2, i.e.,

$$G_{f\text{-PLA}} = (G_f \times W_{PLA\text{-gel}})/W_{PLA\text{-TPV}} \times 100\% \quad (2)$$

where $W_{PLA\text{-gel}}$ and $W_{PLA\text{-TPV}}$ are the weight fraction of PLA phase in the overall gel and in the initial TPV, respectively. Three specimens of each sample were examined and an average value was presented. The gel fraction of the EVA phase ($G_{f\text{-EVA}}$) is measured by the same method.

With an assumption of volume additivity of gel and absorbed solvent during swelling, the swelling ratio (S) of the TPV gel was calculated using eq 3,[20] i.e.,

$$S = 1 + \frac{M_s}{\rho_s}\Big/\left(\frac{W_{PLA\text{-gel}} \times M_2}{\rho_{PLA}} + \frac{W_{EVA\text{-gel}} \times M_2}{\rho_{EVA}}\right) \quad (3)$$

where ρ_{PLA} and ρ_{EVA} are the density of PLA and the solvent, respectively. M_s is the weight of absorbed solvent, i.e., $M_s = M_1 - M_2$.

Thermal Gravimetric Analysis (TGA). TGA (1100SF, Mettler-Toledo International Trade Co., Ltd. Switzerland) was used to evaluate the thermal decomposition behavior of the gel and the degraded TPV. The TGA measurements were performed from 20 to 600 °C at 10 °C/min in nitrogen atmosphere.

Transmission Electron Microscopy (TEM). The morphology evolution of the PLA/EVA-based TPV was studied using an FEI Tecnai G2 TEM at an accelerating voltage of 120 kV. The samples were cryo-microtomed to a section in 80−100 nm thickness at −70 °C using a Leica Ultracut UC6 before TEM observation.

Fourier Transform Infrared (FT-IR). The samples before and after degradation were analyzed on FT-IR spectrometers (Nicolet 6700, USA) in an attenuated total reflection mode (ATR). The final spectrum of each sample was an average of 32 scans at a resolution of 4 cm^{-1} in the wavenumber range of 400−4000 cm^{-1}.

Rheological Behavior. Dynamic rheological experiments were carried out on a DHR-2 rheometer (TA Instruments, USA) in a plate−plate configuration (25 mm in diameter and 1 mm in gap) at 170 °C. The samples were tested in a frequency-sweep mode (from 100 to 0.01 Hz) with a strain of 1%. The strain was predetermined from a strain-sweep experiment to make the measurements in a linear viscoelastic strain range.

Dynamic Mechanical Analysis (DMA). DMA (Q800, TA Instruments, USA) measurement on the TPV was carried out in a tensile-film mode. The specimens (15 × 5.3 × 0.5 mm^3) were tested under a nitrogen atmosphere from −80 to +120 °C at a temperature ramp of 3 °C/min. The frequency and amplitude were set as 1 Hz and 20 μm, respectively. The storage modulus and loss modulus were recorded as a function of temperature.

Mechanical Properties. Tensile properties of the PLA/EVA-based TPV were measured by using a tensile tester (Instron 5967, USA) at a crosshead speed of 200 mm/min.[17] The dimension of the parallel section of the tensile bar is 25 × 4 × 1 mm. Five specimens of each sample were tested and the averaged results were presented. The tensile permanent set (S_p) of each specimen was measured according to eq 4, i.e.,

$$S_p = (L_1 - L_0)/L_0 \times 100\% \quad (4)$$

DOI: 10.1021/acssuschemeng.5b00462
ACS Sustainable Chem. Eng. 2015, 3, 2211−2219

Scheme 1. Illustration of the Main Reactions in the PLA/EVA Blends in the Presence of 2,5-Dimethyl-2,5-di(*tert*-butylperoxy)hexane (AD)

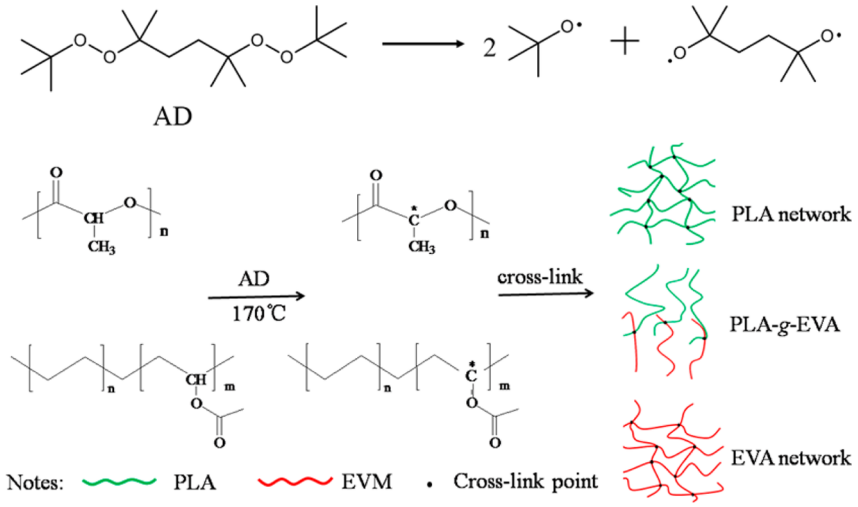

where L_0 is the original length of the parallel section, whereas L_1 is the final length of the stretched parallel section measured 24 h after fracture. The Shore D hardness was measured according to GB/T 531.1-2008. All the mechanical tests were performed at room temperature.

Degradation Behavior. Small pieces of each sample with similar geometry (1.0 mm in thickness) were subjected to *in vitro* degradation. More than ten pieces of each sample were sealed in different reagent bottles, respectively, filled with the same volume of NaOH solution (0.01 mol/L). The degradation experiments were performed at 25 °C in thermostatic water bath. All the samples were dried and weighted (m_0) before the experiments. The samples were taken out weekly and washed with distilled water at different degradation times. The washed samples were weighed (m_i) after complete drying in a vacuum oven at 60 °C for 12 h. The degradation rate (D_r) of the samples was calculated via eq 5:

$$D_R = (m_0 - m_i)/m_0 \times 100\% \quad (5)$$

where m_0 is the weight of the samples before degradation and m_i is the dry weight of the degraded samples with a degradation time of i weeks. Furthermore, the erode morphology of the samples before and after 14 week degradation was observed by using an optical microscope (Axio Scope 1, Zeiss, Germany) in a reflection mode.

RESULTS AND DISCUSSION

Cross-Link of the PLA/EVA-based TPV in the Presence of AD. The 2,5-dimethyl-2,5-di(*tert*-butylperoxy)hexane (AD) could decompose at elevated temperatures, leading to free radicals, as shown on the top of Scheme 1. Both PLA and EVA can form macroradicals via hydrogen abstraction mechanism in the presence of free radicals leading to cross-linked structures.[21,22] PLA-*g*-EVA copolymers may also occur at the interface via a combination of PLA and EVA macroradicals. As a consequence, complex reaction products could be obtained including cross-linked EVA, cross-linked PLA and cross-linked PLA−EVA, as schematically illustrated in Scheme 1. Some side reactions such as branching and degradation were not discussed in this study.

The cross-linked components, gel, in the PLA/EVA-based TPV are insoluble in solvent. The structure and composition of the gel are important to phase morphology and mechanical properties of the TPV, thus they were first studied by swelling equilibrium experiments, as described in the Characterization section.

The overall gel fraction of the TPV (G_f) and the swelling ratios (S) of the gel as a function of AD content are plotted in Figure 1. As expected, the G_f increased with increasing the AD

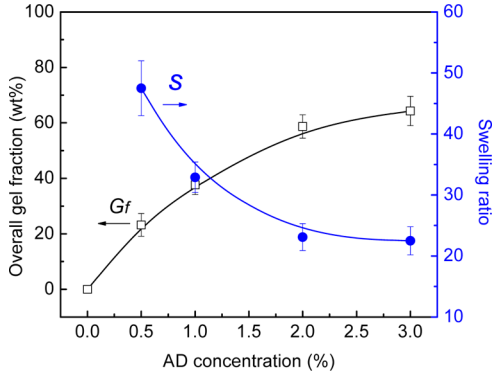

Figure 1. (a) Overall gel fraction (G_f) and (b) swelling ratio (S) of the PLA/EVA-based TPV as a function of AD concentration.

content whereas the S values followed an opposite trend. It is known that the S value is inversely proportional to the cross-link density, thus the cross-link density increased with the AD content.

The TPV gel contains PLA and EVA molecules because both of them were involved in the free radical reactions. Such reaction at the interface is beneficial to the compatibility leading to improved properties.[18,23] Thermal gravimetric analysis (TGA) was performed to characterize the gel composition and the results are shown in Figure 2. The EVA exhibits two-step decomposition corresponding to the CH_3COO- side chain at 335−380 °C and the $-CH_2-CH_2-$ backbone at 445−500 °C, respectively.[24] On the other hand, PLA decomposed sharply in a single step at 340−380 °C. Therefore, the mass residual of the gel at 380 °C is regarded as the backbone of the EVA component whereas the mass lose at this temperature is referred to the combination of PLA and side chain of the EVA. Then the weight fraction of EVA and PLA in the overall gel (i.e., $W_{PLA\text{-}gel}$ and $W_{EVA\text{-}gel}$) is figured out and shown in Figure 3a and the detailed calculation method is shown in the Supporting Information. Obviously, the $W_{EVA\text{-}gel}$ decreases monotonically with the AD concentration whereas the $W_{EVA\text{-}gel}$

DOI: 10.1021/acssuschemeng.5b00462
ACS Sustainable Chem. Eng. 2015, 3, 2211−2219

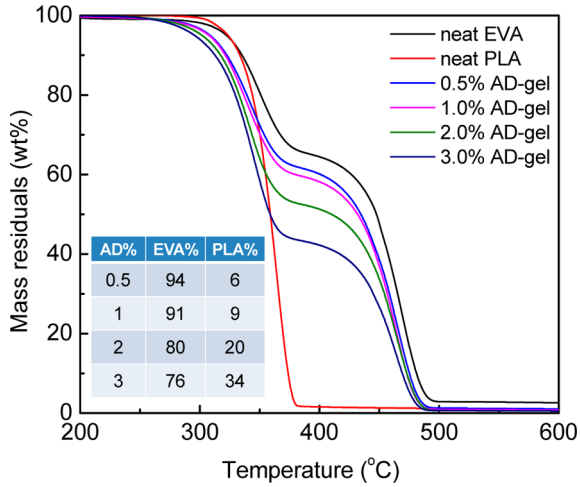

Figure 2. TGA curves of the PLA, EVA and PLA/EVA-based TPV.

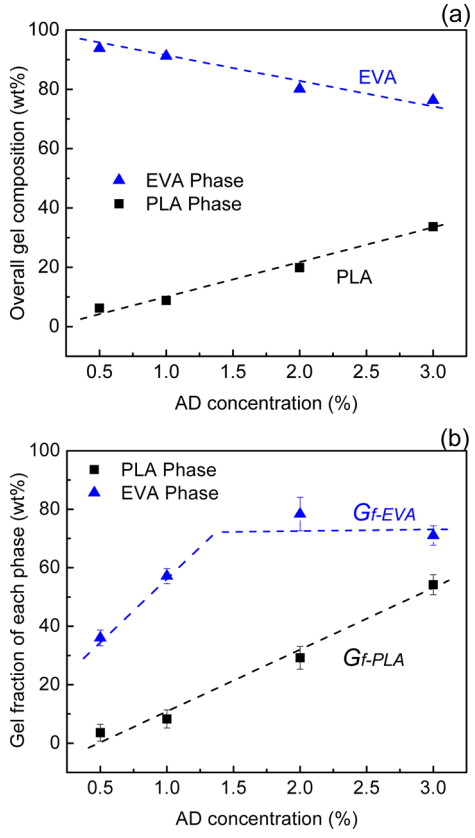

Figure 3. (a) Content of PLA and EVA in the overall gel and (b) individual gel fraction of the PLA ($G_{f\text{-}PLA}$) and EVA ($G_{f\text{-}EVA}$) phases in the PLA/EVA-based TPV.

follows an opposite trend. In the meanwhile, the weight ratio of EVA to PLA ($W_{PLA/EVA}$) in the overall gel drops from 15.1 to 2.3.

The individual gel fraction of the PLA ($G_{f\text{-}PLA}$) and the EVA ($G_{f\text{-}EVA}$) phases was calculated from the overall gel fraction (G_f), the $W_{PLA/EVA}$ values and the initial composition of the TPV via eq 2. The detailed calculation method is shown in the Supporting Information, and the results are plotted in Figure 3b. The PLA and EVA deserved the same contacting possibility with free radicals because the AD was feed into homogeneous PLA/EVA compounds in a single step. The $G_{f\text{-}PLA}$ increased linearly with the AD concentration. However, the $G_{f\text{-}EVA}$ increased sharply with the AD concentration up to 2 wt % and then leveled off. Such reaction of EVA tends to a saturated state when amount of free radical reaches to a certain level. It is also seen from Figure 3b that the individual gel fraction of the EVA phase is always higher than that of the PLA phase in the examined AD range. The gel analysis in Figures 1 and 3 demonstrates that EVA is more aggressive with free radicals.

Morphology Evolution of the PLA/EVA-based TPV. Morphology evolution of the PLA/EVA-based TPV was studied by using transmission electron microscopy (TEM), as shown in Figure 4. As expected, a typical sea−island structure was observed in the physical PLA/EVA (40/60) blend (Figure 4a). The dispersed domains in Figure 4a correspond to the PLA phase which is proven by dynamic mechanical analysis (DMA), see the Discussion section below. The dispersed PLA domains subsequently coalesced and resulted in a dual-continuous morphology when 0.5 wt % of AD was incorporated (Figure 4b). Interestingly, a phase inversion was observed at 1 wt % of AD where the EVA became the dispersed domains (i.e., bright phase in Figure 4c). Such morphology is typical for conventional TPV, e.g., dynamically cross-linked PP/EPDM and PP/NR system where the cross-linked rubber behaves as dispersed domains.[5,25] Surprisingly, the cross-linked EVA domains turned into a dual-continuous phase again with further increasing the AD concentration to 2 wt % (Figure 4d). Chen et al.[26] recently reported PLA/NR-based TPV with continuous cross-linked NR and dispersed PLA phases. The continuity of NR was ascribed to its high viscosity and consequently no rupture in compounding. Apparently, the cross-linked EVA phase in this study is deformable and rupturable which is thus different from the reported PLA/NR system.

Jordhamo et al.[27] developed an empirical model based on the melt-viscosity ratio of dispersed phase to matrix (η_1/η_2) and the volume fractions (ϕ) of each phase to predict the phase inversion region in immiscible binary polymer blends. According to this model, phase inversion would occur when eq 6 holds

$$\frac{\phi_1}{\phi_2} \times \frac{\eta_2}{\eta_1} \approx 1 \tag{6}$$

Jordhamo's model, however, is limited to low shear rates and constant interfacial tension between the phases, thus does not always predict the region of phase inversion correctly.[28,29] Chen and Su ascribed this discrepancy to the fact that the eq 6 overestimates the volume fraction of the high viscosity phase, and then proposed an alternative eq 7,[29] i.e.,

$$\frac{\phi_{hv}}{\phi_{lv}} = 1.2\left(\frac{\eta_{hv}}{\eta_{lv}}\right)^{0.3} \tag{7}$$

where the subscripts "hv" and "lv" denote the high and the low viscosity phase, respectively.

Blending physics dictates that the component with lower viscosity and larger volume tends to be continuous in a binary blend. In the PLA/EVA-based TPV system, the volume ratio of PLA/EVA (60/40) is constant, i.e., $\phi_{PLA}/\phi_{EVA} = 1/2$ (ρ_{PLA} = 1.25 g/cm^3 and ρ_{EVA} = 0.93 g/cm^3). Then the phase inversion is heavily dominated by the viscosity ratio of the EVA and the PLA phases, i.e., η_{EVA}/η_{PLA}. The viscosity of PLA is far higher than that of the EVA at the processing temperature (η_{EVA}/η_{PLA}

DOI: 10.1021/acssuschemeng.5b00462
ACS Sustainable Chem. Eng. 2015, 3, 2211−2219

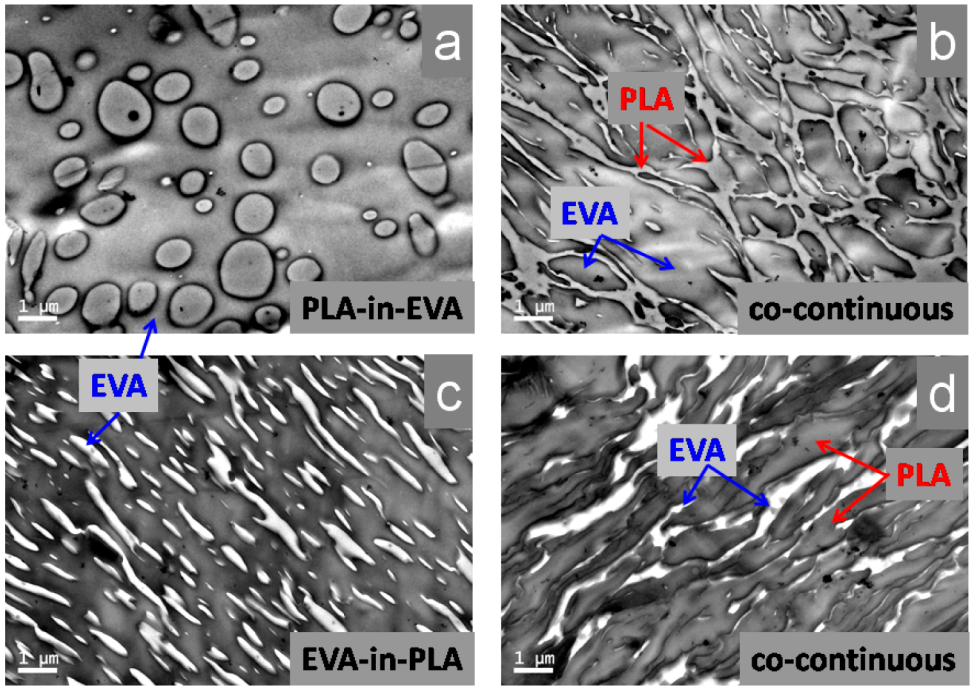

Figure 4. TEM images (scale bar = 1.0 μm) of the PLA/EVA-based TPV by using the following amount of AD as a cross-linking agent: (a) 0.0 wt %, (b) 0.5 wt %, (c) 1.0 wt % and (d) 2.0 wt %. The EVA and PLA phases are labeled.

≈ 1/3 in the frequency zone of 1−100 Hz), as shown in Figure 5. Thus, EVA is the continuous phase in the PLA/EVA (40/60)

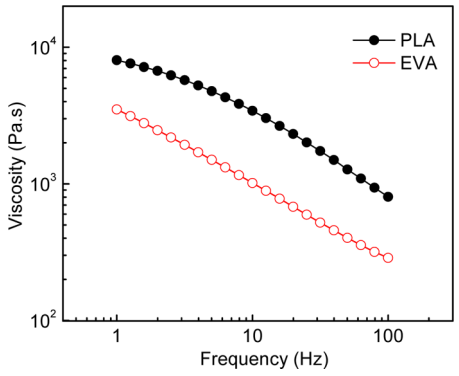

Figure 5. Complex viscosity of the PLA and the EVA at the processing temperature as a function of frequency.

blend with dispersed PLA domains (Figure 4a). A phase inversion was expected to take place at a η_{EVA}/η_{PLA} ratio of 2−5.4 according to Jordhamo's and Chen's models, which occurred at around 1 wt % of AD in this study (Figure 4c). Because the individual cross-linked fraction of the EVA phase ($G_{f\text{-}EVA}$) initially increased faster and then slowed down with increasing the AD concentration (Figure 3) whereas the $G_{f\text{-}PLA}$ increased linearly, it would result in a decrease in η_{EVA}/η_{PLA} at higher AD concentration which drives the continuity of the EVA phase again (Figure 4d). In addition, a gel comprising both of the EVA and PLA should exist in the TPVs, notably at the interface of the PLA and EVA phases, which as compatibilizer is beneficial to fineness of the morphology and interfacial adhesion.

To summarize, the morphology evolution in the PLA/EVA-based TPV is dominated by the variation of viscosity ratio between the PLA and EVA phases.

Dynamic Mechanical analysis (DMA). The DMA was used to study dynamic mechanical thermal properties of the PLA/EVA-based TPV, as shown in Figure 6. The tan δ peak temperature is referred to as glass transition (T_g) in this work. Two T_g values of the PLA/EVA-based TPV are distinguished upon heating, i.e., $T_{g\text{-}EVA}$ around −20 °C and $T_{g\text{-}PLA}$ around +60 °C. Neither $T_{g\text{-}EVA}$ nor $T_{g\text{-}PLA}$ was influenced obviously by the dynamic cross-link indicating indirectly a low cross-link density. The $T_{g\text{-}EVA}$ in the TPV with 1.0 wt % AD is 2 °C lower than the others, which is ascribed to a variation of EVA phase from (co)continuity to dispersion.[19,30] EVA50 is a random copolymer with an average VA content of 50 wt % in the copolymer. In practice, the VA content may be different for every chain and the sequence of monomers may not be perfectly random in a single chain. This might result in VA-reach chains or VA-reach segments in the EVA50 materials. It is known that PLA is miscible with poly(vinyl acetate) (PVAc) and ethylene-*co*-vinyl acetate (EVA) with VA content of >85 wt % but not miscible with poly(ethylene). Therefore, VA segments or VA-rich chains in the EVA50 domains prefer to move to the interface and miscible with PLA component during blending. As a consequence, the ethylene content inside of the EVA50 domains would be higher than 50 wt %, resulting in a lower T_g value of EVA50. This effect only becomes obvious when the domain size is small enough. However, direct experimental evidence of this proposal is still lacking.

Amorphous polymeric materials are generally stiff in glassy state and become soft above the T_g. In combination with microscopy techniques, the DMA results can be used to determine the morphology evolution. The storage modulus (E') of the PLA/EVA blend is as low as 10 MPa at 25 °C, which is between $T_{g\text{-}EVA}$ and $T_{g\text{-}PLA}$; however, it is above 200 MPa for the cross-linked PLA/EVA blends (Figure 6b). These results confirm that PLA is the dispersed phase in the PLA/EVA blend and is continuous after incorporation of 0.5−2.0 wt % of the AD. In addition, the E' values of the TPV with 0.5 and

DOI: 10.1021/acssuschemeng.5b00462
ACS Sustainable Chem. Eng. 2015, 3, 2211−2219

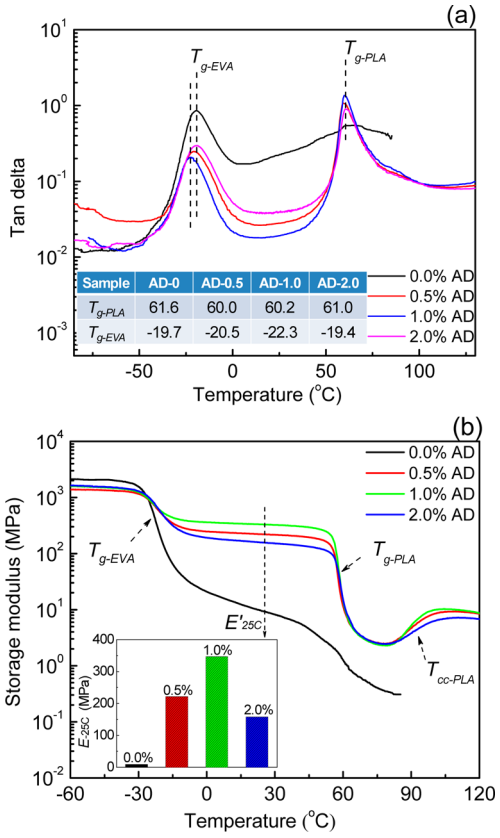

Figure 6. Dynamic mechanical thermal analysis of the PLA/EVA-based TPV as a function of AD concentration and temperature: (a) tan δ and (b) storage modulus (E'). The T_g of PLA and EVA in the TPV are inserted in panel a. The E' values at 25 °C (E_{25C}) are plotted as a function of AD concentration and inserted in panel b.

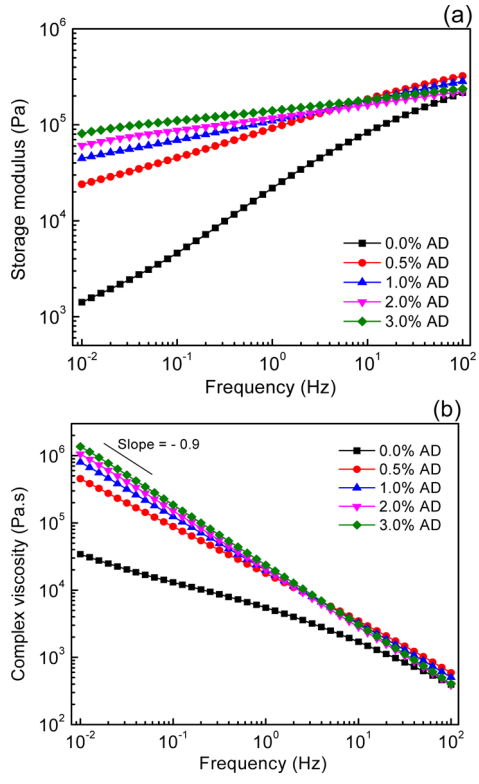

Figure 7. Storage modulus (G') and complex viscosity (η^*) of the PLA/EVA-based TPV as a function of frequency and AD content.

2.0 wt % AD are obviously lower than those of the TPV with 1.0 wt % AD, which is also correlated to the morphology evolution (see the TEM section, Figure 4b,d). Increases in E' of the TPV due to the cold crystallization of PLA phase ($T_{cc\text{-}PLA}$) are detected at around 100 °C, indicating an amorphous feature of the samples.

Rheological Behavior. Rheology is a powerful technique to study structures of polymeric materials. The storage modulus (G') and complex viscosity (η^*) of the PLA/EVA-based TPV melts as a function of AD concentration and frequency (ω) are shown in Figure 7a,b, respectively. Both the G' and the η^* of the PLA/EVA blend were enhanced considerably after addition of 0.5 wt % AD, and the values were increased further but less pronounced with increasing the AD concentration from 0.5 wt % to 3.0 wt %. Meanwhile, the dynamically cross-linked PLA/EVA melts exhibit solid-like behavior at low frequency zone, i.e., indistinctive dependence of G' on frequency and high slope (−0.9) of $\log(\eta^*)$ vs $\log(\omega)$, demonstrating the existence of cross-link and/or branching network (see Scheme 1 and Figure 1). On the other hand, the rheological data indicate melt processability of the TPV notably at high frequency zone.

Mechanical Properties. The AD content has vital effect on the mechanical properties of the PLA/EVA-based TPV, as shown in Figure 8a,b. The stress−strain behavior of the PLA/EVA blend with and without cross-link is inserted in Figure 8a. The PLA/EVA blend has high elongation at break ($\varepsilon_b \approx 600\%$) but low tensile strength ($\sigma_t \approx 8$ MPa) and tensile modulus (small initial slope of the stress−strain curve) which is more like an uncured EVA rubber. After addition of AD, the samples show higher tensile modulus, reasonable elongation at break and more pronounced strain hardening. The σ_t was increased from 8 to 21 MPa with the AD content up to 1 wt % (Figure 8a) whereas the ε_b decreased to 210%. The ε_b and storage modulus (E', room temperature) of PP/EPDM(40/60)-based TPV were reported up to 120% and 150 MPa, respectively,[31] which are lower in comparison with the PLA/EVA-based TPV. Tensile set (T_s) and hardness are also important for TPV application. Low T_s values indicate high elastic recovery. The T_s values of the physical PLA/EVA blend is 90% which is reduced by approximately 65% after the dynamic cross-link regardless of the AD concentration (Figure 8b). In addition, the Shore D hardness of the PLA/EVA blend was enhanced from 14 to 50 after addition of the AD and kept constant with AD concentration. Therefore, the mechanical behavior is strongly correlated to the cross-link structure and phase morphology of the TPV. Moreover, the existence of PLA-*g*-EVA, notably at the interface of the PLA and EVA components, is beneficial to the mechanical properties of the TPV as well.

***In Vitro* Degradation Behavior of the PLA/EVA-based TPV.** The degradation rate of polyesters is affected by the medium, temperature and molecular structures, etc.[32] The *in vitro* degradation behavior of PLA, EVA and PLA/EVA-based TPV, in an aqueous alkali at 25 °C, were studied by means of degradation rate, molecular structure and morphological analysis as a function of time.

The weight changes of the PLA/EVA-based TPV during degradation were monitored, and the degradation rate (D_r, defined in the Characterization section) is plotted as a function of time in Figure 9a. Apparently, the PLA showed faster degradation than the other samples, but hardly any weight loss of the EVA was detected. The degradation rate of the TPV

DOI: 10.1021/acssuschemeng.5b00462
ACS Sustainable Chem. Eng. 2015, 3, 2211−2219

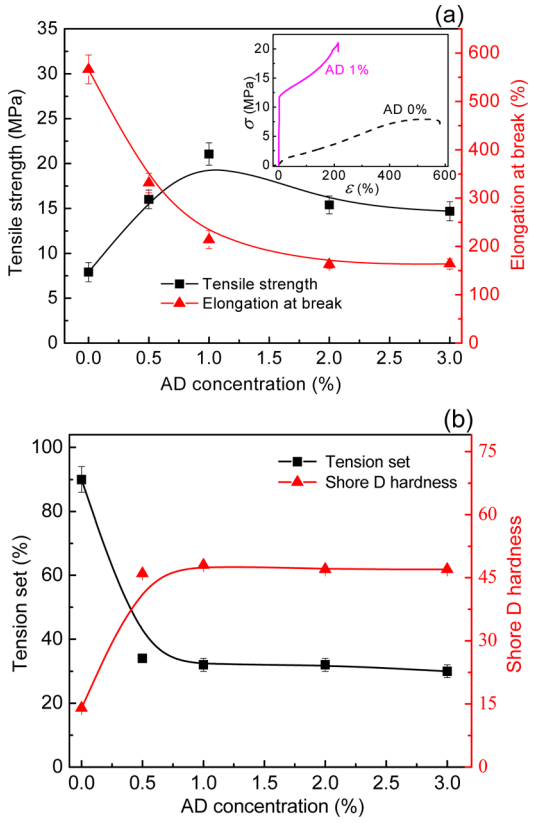

Figure 8. Mechanical properties of the PLA/EVA-based TPV as a function of AD concentration: (a) tensile strength and elongation at break and (b) tensile set and hardness. The stress−strain curves of the PLA/EVA blend and the PLA/EVA-based TPV with 1.0 wt % AD are inset in panel a.

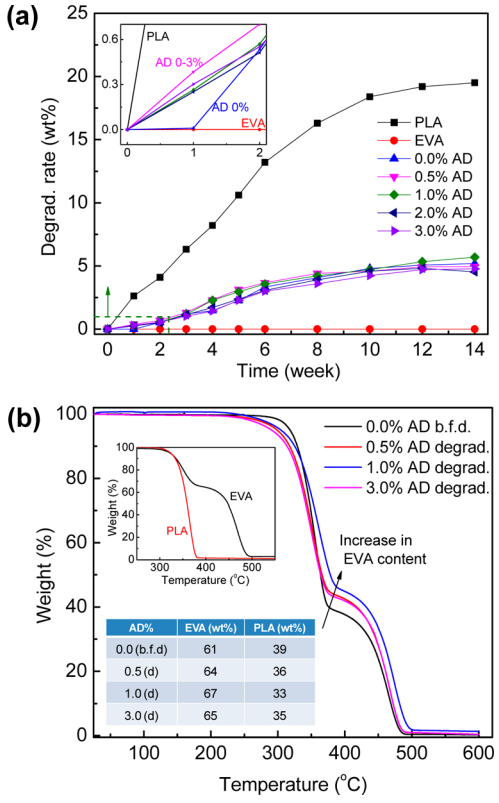

Figure 9. (a) Degradation rate of the PLA, EVA and PLA/EVA-based TPV as a function of degradation time. The degradation rate in the first 2 weeks is enlarged as an inset in panel a. (b) TGA curves of the 14 week degraded TPV in comparison with the nondegraded physical PLA/EVA blend. TGA curves of PLA and EVA as a reference and the compositions of the examined samples are inset in panel b. The abbreviation of b.f.d. means before degradation.

increased gradually during the first 10 weeks and then leveled off. A similar transition point (~6 weeks) was observed in PLA/PBAT systems as well where the experiment was carried out at 60 °C.[21] An overall degradation rate of the TPV approached to approximately 5 wt % within 10 weeks. The degradation percentage of the PLA phase is expected to be around 12.5 wt % assuming that EVA is stable, which is lower than that of the neat PLA (around 18 wt %). Hence the EVA restricted the degradation of PLA to a certain extent. It is worth to note that the physical PLA/EVA blend and the cross-linked TPV showed different degradation behavior in the initial stage, as enlarged in Figure 9a. The cross-linked TPV showed notable weight lose (0.4 wt %) already within the first week whereas the degradation rate of the physical PLA/EVA blend was still close to zero. The PLA domains were embedded in the EVA matrix in the physical blend and time was required for the migration of aqueous alkali into the PLA phase, thus indistinctive degradation during the first week. Degradation was then triggered once the aqueous alkali went into the PLA domains. The PLA/EVA blends exhibited similar degradation behavior after an induction period regardless of AD concentration.

The composition of degraded samples was analyzed by using TGA, as shown in Figure 9b. The degradation rate calculated from Figure 9b is slightly larger than 5 wt % based on the proposed degradation of the sole PLA component, which supported the above discussion. Both PLA and EVA possess ester groups (−RCOOR′−) and the *in vitro* degradation in aqueous alkali is regarded as breakages of ester groups. The degradation behavior of the PLA/EVA-based TPV was further investigated by FT-IR in a molecular level, as shown in Figure 10. The ester groups of PLA and EVA exhibit absorption bands

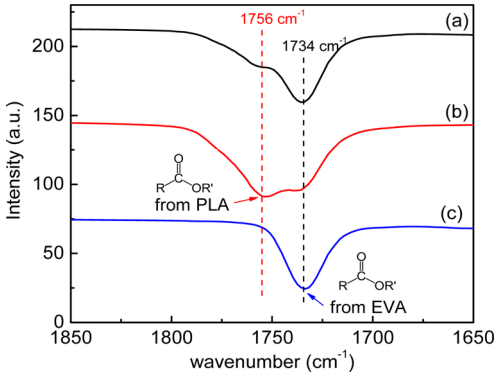

Figure 10. FT-IR spectra of the PLA/EVA-based TPV with (a) AD 0.0 wt % before degradation, (b) AD 1.0 wt % before degradation and (c) AD 1.0 wt % after degradation. The measurement was carried out in ATR mode.

at 1756 and 1734 cm^{-1}, respectively.[33,34] The FT-IR band at 1734 cm^{-1} is dominant in the physical PLA/EVA blend whereas the band at 1734 cm^{-1} behaves as a shoulder because EVA is the continuous phase (spectrum a). An opposite result is observed in the TPV with 1.0 wt % AD due to a phase inversion (spectrum b). Interestingly, the dominant peak (1756 cm^{-1}) in the spectrum b disappeared after degradation of the

DOI: 10.1021/acssuschemeng.5b00462
ACS Sustainable Chem. Eng. 2015, 3, 2211−2219

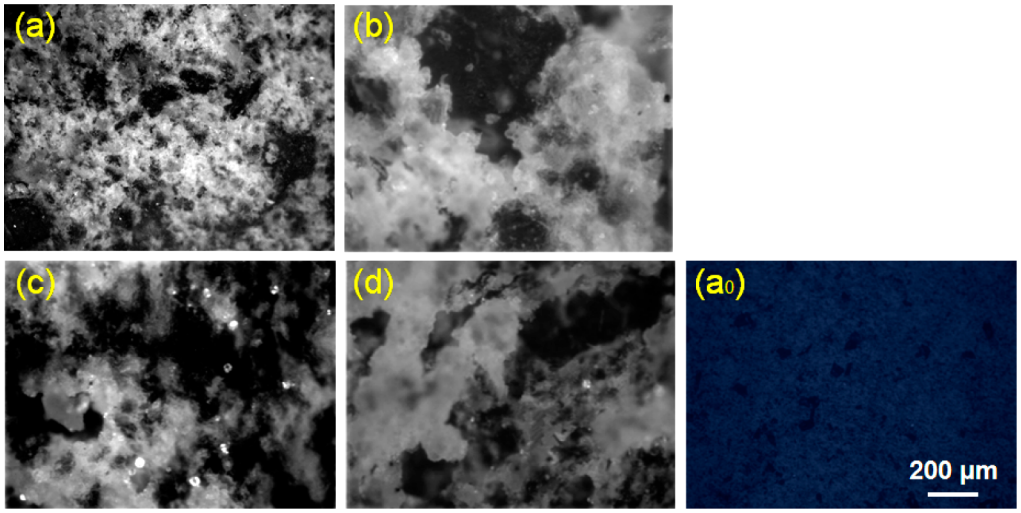

Figure 11. Optical microscopy images (same magnification) of the surfaces of PLA/EVA-based TPV. The images a, b, c and d correspond to the degraded PLA/EVA blends with AD concentration of 0.0, 0.5, 1.0 and 2.0 wt %, respectively. The image a_0 corresponds to the image a before degradation whereas the superficial morphology of the other samples before degradation is similar to the image a_0 thus not present.

samples (spectrum c). The FT-IR spectra via ATR mode mainly examine the top layer of the samples. Therefore, these results convincingly prove the complete degradation of PLA in the surface layer of the TPV whereas the side ester groups of the EVA are retained.

The superficial morphology of the PLA/EVA-based TPV before and after degradation was observed by using optical microscopy (OM) in reflection mode, as shown in Figure 11. The surfaces of different samples are smooth before degradation, taking the PLA/EVA blend as an example, as shown in Figure 11a_0. Erosion of the samples was clear after degradation. The dark phase in Figure 11a–d corresponds to the degraded PLA component leaving holes on the surfaces whereas the bright phase refers to the EVA. Small dark domains are observed in Figure 11a, which become much bigger in the case of PLA/EVA-AD0.5% sample (Figure 11b) and become even continuous with increasing the AD concentration (Figure 11c,d). These results further evidenced that (i) degradation of PLA phase occurred rather than EVA phase and (ii) phase inversion with increasing the AD concentration. Thus, the OM images well support the above discussion in the phase morphology and degradation mechanism. It has to remark that the OM image with low magnification demonstrated the surfaces of the compression molded TPV after degradation in aqueous alkali and some EVA particles may already be gone when the matrix is dissolved, resulting in some differences between these images and the above TEM images.

CONCLUSIONS

Partially biobased and degradable thermoplastic vulcanizates (TPV) were successfully fabricated by dynamic cross-link of 40 wt % of poly(lactide) (PLA) and 60 wt % of ethylene-*co*-vinyl acetate (EVA) with different amount of 2,5-dimethyl-2,5-di(*tert*-butylperoxy)hexane (AD). The EVA reacted with AD faster than PLA leading to a sharper increase in the individual gel content of the EVA phase which, however, slowed down at the AD content higher than 1.0 wt %. On the other hand, the individual gel content of the PLA phase increased linearly with AD content up to 3.0 wt %. The competition in reactivity results in variation of their viscosity ratios, i.e., η_{PLA}/η_{EVA}, which further influenced the phase morphology. As a consequence, the phase morphology of the PLA/EVA blends evolved from a sea–island-type structure to dual-continuous morphology, then to an island–sea-type structure (phase inversion) and finally dual-continuous morphology again with increasing the AD content from 0.0 to 3.0 wt %. The dynamic cross-link and phase evolution enhanced the elasticity (G') and viscosity (η^*) of the PLA/EVA melts showing solid-like behavior at low frequency. The storage modulus (E') of the physical PLA/EVA blends at room temperature was increased dramatically after dynamic cross-link due to the continuity of PLA phase. Meanwhile, superior mechanical properties of the TPV, e.g., high tensile strength (σ_t = 21 MPa), low tensile set (T_s = 30%) and moderate elongation (ε_b = 210%) and storage modulus (E' = 350 MPa) were achieved at 1.0 wt % of the AD. The *in vitro* degradation results showed degradability of the PLA/EVA-based TPV in aqueous alkali at room temperature and the degradation behavior is influenced by the phase morphology as well, notably in the initial stage. A degradation rate of around 5 wt % was reached within 10 weeks and it leveled off in the subsequent weeks. TGA, FT-IR and optical microscopy results convincingly indicated that it was the PLA phase degraded rather than the EVA phase. To summarize, degradable and partially biobased PLA/EVA-based TPV with superior mechanical performance and novel phase morphology are obtained by dynamic cross-link with 2,5-dimethyl-2,5-di(*tert*-butylperoxy)hexane, which appear suited for substitution of traditional TPV.

ASSOCIATED CONTENT

Supporting Information

The calculation method of individual gel fraction of the PLA ($G_{f\text{-}PLA}$) and the EVA ($G_{f\text{-}EVA}$) phases. The Supporting Information is available free of charge on the ACS Publications website at DOI: 10.1021/acssuschemeng.5b00462.

(PDF)

AUTHOR INFORMATION

Corresponding Authors

*P. Ma. E-mail: p.ma@jiangnan.edu.cn. Tel.: +86 510 85917019.

DOI: 10.1021/acssuschemeng.5b00462
ACS Sustainable Chem. Eng. 2015, 3, 2211–2219

*M. Chen. E-mail: mq-chen@jiangnan.edu.cn. Tel.: +86 510 85917019.

Notes

The authors declare no competing financial interest.

■ ACKNOWLEDGMENTS

This work is supported by the National Natural Science Foundation of China (51303067, 51573074) and Natural Science Foundation of Jiangsu Province (BK20130147).

■ REFERENCES

(1) Wu, J.-H.; Li, C.-H.; Chiu, H.-T.; Shong, Z.-J.; Tsai, P.-A. Anti-vibration and vibration isolator performance of poly (styrene-butadiene-styrene)/ester-type polyurethane thermoplastic elastomers. *Polym. Adv. Technol.* **2010**, *21*, 164−169.

(2) Dey, P.; Naskar, K.; Dash, B. Thermally cross-linked and sulphur-cured soft TPVs based on S-EB-S and S-SBR blends. *RSC Adv.* **2014**, *4*, 35879−35895.

(3) Wu, H.; Tian, M.; Zhang, L. New understanding of morphology evolution of thermoplastic vulcanizate (TPV) during dynamic vulcanization. *ACS Sustainable Chem. Eng.* **2014**, *3*, 26−32.

(4) Wu, H.; Tian, M.; Zhang, L. New understanding of micro-structure formation of the rubber phase in thermoplastic vulcanizates (TPV). *Soft Matter* **2014**, *10*, 1816−1822.

(5) Naskar, K.; Gohs, U.; Wagenknecht, U. PP-EPDM thermoplastic vulcanisates (TPVs) by electron induced reactive processing. *eXPRESS Polym. Lett.* **2009**, *3*, 677−683.

(6) Mirzadeh, A.; Lafleur, P. G.; Kama, M. R. The effect of compatibilizer on the co-continuity and nanoclay dispersion level of nanocomposites based on PP/EPDM. *Polym. Eng. Sci.* **2010**, *50*, 2131−2142.

(7) Mondal, M.; Gohs, U.; Wagenknecht, U. Additive free thermoplastic vulcanizates based on natural rubber. *Mater. Chem. Phys.* **2013**, *143*, 360−366.

(8) Kalkornsurapranee, E.; Nakason, C.; Kummerlöwe, C. Development and preparation of high-performance thermoplastic vulcanizates based on blends of natural rubber and thermoplastic polyurethanes. *J. Appl. Polym. Sci.* **2013**, *128*, 2358−2367.

(9) Wu, W.; Wan, C.; Zhang, Y. Graphene oxide as a covalent-crosslinking agent for EVM-g-PA6 thermoplastic elastomeric nanocomposites. *RSC Adv.* **2015**, *5*, 39042−39051.

(10) l'Abee, R.; Goossens, H. Sub-micrometer thermoplastic vulcanizates obtained by reaction-induced phase separation of miscible mixtures of poly(ethylene) and alkyl methacrylates. *Eur. Polym. J.* **2009**, *45*, 503−514.

(11) Razmjooei, F.; Naderi, G.; Bakhshandeh, G. Preparation of dynamically vulcanized thermoplastic elastomer nanocomposites based on LLDPE/reclaimed rubber. *J. Appl. Polym. Sci.* **2012**, *124*, 4864−4873.

(12) Rasal, R. M.; Janorkar, A. V.; Hirt, D. E. Poly (lactic acid) modifications. Hirt. *Prog. Polym. Sci.* **2010**, *35*, 338−356.

(13) Yuan, D.; Chen, K.; Xu, C. Crosslinked bicontinuous biobased PLA/NR blends via dynamic vulcanization using different curing systems. *Carbohydr. Polym.* **2014**, *113*, 438−445.

(14) Liu, G. C.; He, Y. S.; Zeng, J. B. Fully biobased and supertough polylactide-based thermoplastic vulcanizates fabricated by peroxide-induced dynamic vulcanization and interfacial compatibilization. *Biomacromolecules* **2014**, *15*, 4260−4271.

(15) Šturcová, A.; Davies, G. R.; Eichhorn, S. J. Elastic modulus and stress-transfer properties of tunicate cellulose whiskers. *Biomacromolecules* **2005**, *6*, 1055−1061.

(16) Joubert, C.; Cassagnau, P.; Michel, A. Influence of the processing conditions on a two-phase reactive blend system: EVA/PP thermoplastic vulcanizate. *Polym. Eng. Sci.* **2002**, *42*, 2222−2233.

(17) Wu, W.; Wan, C.; Wang, S. Reactive processing of ethylene-vinyl acetate rubber/polyamide blends via a dynamic transesterification reaction. *Polym. Bull.* **2014**, *71*, 1505−1521.

(18) Ma, P.; Hristova-Bogaerds, D. G.; Goossens, J. G. P. Toughening of poly (lactic acid) by ethylene-co-vinyl acetate copolymer with different vinyl acetate contents. *Eur. Polym. J.* **2012**, *48*, 146−154.

(19) Ma, P.; Xu, P.; Liu, W. Bio-based poly (lactide)/ethylene-co-vinyl acetate thermoplastic vulcanizates by dynamic crosslinking: structure vs. property. *RSC Adv.* **2015**, *05*, 15962−15968.

(20) Amin, M.; Nasr, G. M.; Attia, G. Determination of the crosslink density of conductive ternary rubber vulcanizates by solvent penetration. *Mater. Lett.* **1996**, *28*, 207−213.

(21) Ma, P.; Cai, X.; Zhang, Y. In-situ compatibilization of poly (lactic acid) and poly (butylene adipate-co-terephthalate) blends by using dicumyl peroxide as a free-radical initiator. *Polym. Degrad. Stab.* **2014**, *102*, 145−151.

(22) Bianchi, O.; Martins, J. D. N.; Fiorio, R. Changes in activation energy and kinetic mechanism during EVA crosslinking. *Polym. Test.* **2011**, *30*, 616−624.

(23) Coran, A. Y.; Patel, R. Rubber-thermoplastic compositions. Part IV. thermoplastic vulcanizates from various rubber-plastic combinations. *Rubber Chem. Technol.* **1981**, *54*, 892−903.

(24) Rimez, B.; Rahier, H.; Van, A. G. The thermal degradation of poly (vinyl acetate) and poly (ethylene-co-vinyl acetate), Part I: Experimental study of the degradation mechanism. *Polym. Degrad. Stab.* **2008**, *93*, 800−810.

(25) Mondal, M.; Gohs, U.; Wagenknecht, U. Polypropylene/natural rubber thermoplastic vulcanizates by eco-friendly and sustainable electron induced reactive processing. *Radiat. Phys. Chem.* **2013**, *88*, 74−81.

(26) Chen, Y.; Yuan, D.; Xu, C. Dynamically vulcanized biobased polylactide/natural rubber blend material with continuous cross-linked rubber phase. *ACS Appl. Mater. Interfaces* **2014**, *6*, 3811−3816.

(27) Jordhamo, G. M.; Manson, J. A.; Sperling, L. H. Phase continuity and inversion in polymer blends and simultaneous interpenetrating networks. *Polym. Eng. Sci.* **1986**, *26*, 517−524.

(28) Everaert, V.; Aerts, L.; Groeninckx, G. Phase morphology development in immiscible PP/(PS/PPE) blends influence of the melt-viscosity ratio and blend composition. *Polymer* **1999**, *40*, 6627−6644.

(29) Chen, T. H.; Su, A. C. Morphology of poly (p-phenylene sulfide) polyethylene blends. *Polymer* **1993**, *34*, 4826−4831.

(30) Ma, P.; Hristova-Bogaerds, D. G.; Schmit, P. Tailoring the morphology and properties of poly (lactic acid)/poly (ethylene)-co-(vinyl acetate)/starch blends via reactive compatibilization. *Polym. Int.* **2012**, *61*, 1284−1293.

(31) Brostow, W.; Datashvili, T.; Hackenberg, K. P. Effect of different types of peroxides on properties of vulcanized EPDM/PP blends. *Polym. Compos.* **2010**, *31*, 1678−1691.

(32) Gorrasi, G.; Pantani, R. Effect of PLA grades and morphologies on hydrolytic degradation at composting temperature: Assessment of structural modification and kinetic parameters. *Polym. Degrad. Stab.* **2013**, *98*, 1006−1014.

(33) Ma, P.; Jiang, L.; Ye, T. Melt free-radical grafting of maleic anhydride onto biodegradable poly (lactic acid) by using styrene as a comonomer. *Polymers* **2014**, *6*, 1528−1543.

(34) Ma, P.; Hristova-Bogaerds, D. G.; Schmit, P. Reactive compatibilization of ethylene-co-vinyl acetate/starch blends. *Macromol. Res.* **2012**, *20*, 1054−1062.

DOI: 10.1021/acssuschemeng.5b00462
ACS Sustainable Chem. Eng. 2015, 3, 2211−2219